Search by Return: Stochastic Resetting in Fluctuating Harmonic Potentials

Derek Frydel

Department of Chemistry, Universidad Técnica Federico Santa María, Campus San Joaquin, Santiago, Chile (Dated: November 19, 2025)

We study a class of stochastic resetting (SR) processes in which a diffusing particle alternates between free motion and confinement by an externally controlled potential. When the particle is recaptured, it undergoes a return trajectory that drives it toward a designated reset point. In standard SR, such returns are treated as instantaneous, but in realistic setups they have finite duration and introduce imprecision in the starting points of subsequent search attempts. We analyze a fluctuating harmonic potential in which return trajectories are forcibly terminated the moment the particle reaches the origin, ensuring that all outward (diffusive) trajectories begin from the same point. This is implemented through instantaneous positional information: a feedback signal that shortens the return phase without incurring additional mechanical energetic cost. We examine several search protocols built on this controlled return mechanism and determine their mean first-passage times (MFPTs). Of particular interest is a protocol in which outward diffusion is eliminated entirely and the return motion itself becomes the search mechanism. This "search by return" perspective reverses the conventional logic of SR and yields a closed-form MFPT that highlights the efficiency of using return dynamics as the primary search strategy.

Since its modern formulation, stochastic resetting has drawn growing interest across disciplines— as both an efficient search strategy and a nonequilibrium process. In its canonical form, it describes a random walk that is interrupted and a walker instantly returned to a fixed starting point. Experimentally, this behavior can be approximated using a fluctuating trapping potential that intermittently releases and recaptures a particle. However, such implementations inevitably introduce return trajectories and imprecision in the resetting position. In this work, we examine how to control these return trajectories to ensure that the initial position of a subsequent outgoing trajetory is the same. We then explore a range of search protocols that incorporate return trajectories into the search process.

I. INTRODUCTION

Stochastic resetting (SR) describes a random walk that is intermittently interrupted and returned to its initial position. Although the idea of restarting stochastic dynamics has appeared in several contexts—including search algorithms in computer science [1, 2] and intermittency models in chemical physics [3, 4]— the modern statistical-physics formulation is due to Evans and Majumdar [5], who introduced diffusion with Poissonian resets and uncovered its nonequilibrium stationary state and optimal-resetting properties. Since then, SR has been extended to diverse stochastic processes, confinement geometries, and search strategies [6-19], with comprehensive overviews in [19-22]. Experimental realizations using holographic optical tweezers [23, 24] have further motivated the study of resetting in realistic potentials, especially where finite return times and positional uncertainty become unavoidable.

A natural physical realization of SR is a fluctuating trap that intermittently releases and recaptures a particle [23–25]. This model has attracted interest both as a variant of SR and as a nonequilibrium setup in its own right [25–32]. However, if interpreted strictly as SR, fluctuating traps introduce a struc-

tural complication: *return trajectories*. These returns extend the duration of a reset cycle and introduce imprecision in the starting point of subsequent outgoing trajectories.

The present work investigates a fluctuating trap model in which return trajectories are terminated at the exact moment the particle first reaches the origin, x=0. This enforces a sharp initial condition for outgoing trajectories and converts the return dynamics from a liability into a useful ingredient of the search process. We also explore several search protocols that explicitly incorporate return trajectories, thereby revealing how their structure can be exploited rather than suppressed.

The idea of enforcing return termination at the origin was first introduced in [26] to bring fluctuating-trap models closer to standard SR. A detailed analysis for a linear potential followed in [27]. Return trajectories as active components of the search protocol were subsequently explored in [33], with further development for a linear trap in [34].

Here we focus on a fluctuating *harmonic* trap. Harmonic potentials are the most widely used and experimentally accessible means of implementing controlled SR: optical tweezers, magnetic trapping, and feedback-controlled colloidal setups naturally realize quadratic confinement with tunable stiffness K(t) [35–40]. Because the resulting dynamics reduces to the Ornstein–Uhlenbeck process, relaxation and first-passage properties remain analytically tractable and directly relevant to experiments.

Return trajectories also motivate a conceptual shift. In standard SR, the search occurs during outward diffusion from the origin, while returns are treated as instantaneous. Once return trajectories are made explicit, this logic can be inverted: the return motion itself can serve as the search mechanism. This "search by return" viewpoint is not a special case but a conceptual dual of conventional SR, highlighting that a reset cycle contains two dynamical stages—outgoing and return—either of which may carry the search depending on how the system is controlled.

This paper is organized as follows. Sec. II reviews the fluctuating-trap model and the theoretical tools used throughout. Sec. III applies them to four search protocols, each ex-

ploiting return trajectories differently. Final remarks appear in Sec. IV.

II. THE MODEL

This work considers a Brownian particle in a harmonic potential that is intermittently switched on and off. Fluctuations of the potential prevent a particle from reaching equilibrium, giving rise to a nonequilibrium setup. We refer to the system with the potential turned off as the *off* state, and to the system with the potential turned on as the *on* state.

Trajectories in the "off" state are called *outgoing trajectories*, while those in the "on" state are referred to as *return trajectories*. The overdamped Langevin dynamics governing the motion in each state is given by

$$\dot{x}(t) = \begin{cases} \sqrt{2D} \, \eta(t), & \text{(outgoing)}, \\ -\mu K x(t) + \sqrt{2D} \, \eta(t), & \text{(return)}, \end{cases}$$
(1)

where μ is the mobility, K the trap stiffness, D the diffusion constant, and $\eta(t)$ is a zero-mean, delta-correlated Gaussian white noise with $\langle \eta(t)\eta(t')\rangle = \delta(t-t')$.

The duration of each outgoing trajectory is drawn from an exponential (memoryless) distribution,

$$r(t) \equiv r_{\text{off}}(t) = \frac{1}{\tau} e^{-t/\tau}, \qquad (2)$$

which corresponds to a constant-rate process. As a result, the dynamics is Markovian, despite being irreversible.

Once the potential is switched on, the particle begins to drift toward the trap center. The potential remains on until the particle reaches the origin, x = 0, for the first time. This return mechanism defines the end of the "on" state, and there is no predefined distribution for the return duration $r_{\rm on}(t)$. Instead, $r_{\rm on}(t)$ emerges from the first-passage time distribution of a Brownian particle in a harmonic trap.

This setup ensures that all outgoing trajectories restart from the position at the origin. Physically, such a mechanism could be realized by an "off-switch" located at the origin, which deactivates the potential upon the particle's arrival, or by a feedback control system that instantaneously resets the dynamics upon observing the particle at x=0.

A. steady-state distributions

The Fokker–Planck formulation of the current model has been analyzed in [26]. To avoid redundancy, we adopt here an alternative presentation aligned with the goals of this paper and obtain only the quantities that will be directly used in formulating the mean first passate time (MFPT).

At any time, an ensemble of realizations can be viewed as composed of two subensembles: those evolving while the trap is on and those evolving while the trap is off. Accordingly, $n_{\text{on}}(x,t)$ denotes the probability density of finding the particle at position x at time t given that the trap is on, and $n_{\text{off}}(x,t)$

denotes the corresponding density given that the trap is off. These do not represent different particles but the two dynamical "modes" of the same particle. We next obtain explicit formulas for those distributions under steady-state conditions.

Since outgoing trajectories are associated with free Brownian motion starting from the origin, the time-dependent probability density they give rise to is the standard Gaussian kernel: $p(x,t) = \frac{1}{\sqrt{4\pi Dt}} e^{-x^2/(4Dt)}$. Because outgoing trajectories do not evolve indefinitely but are interrupted (or renewed), the distirbution we need to consider is $S_r(t) p(x,t)$, where $S_r(t) = \int_t^\infty dt' \, r(t')$ is the survival function. The steady-state distribution due to outgoing particles is then obtained by averaging $S_r(t) \, p(x,t)$ over time,

$$n_{\text{off}}(x) = \frac{1}{\tau} \int_0^\infty dt \, S_r(t) \, p(x, t), \tag{3}$$

where τ^{-1} ensures correct normalization. Specific to exponential r(t), we can use the relation $S_r(t) = \tau r(t)$, which simplifies the above expression,

$$n_{\text{off}}(x) = \int_0^\infty dt \, r(t) \, p(x,t) = \frac{1}{\sqrt{D\tau}} e^{-|x|/\sqrt{D\tau}}, \tag{4}$$

which evaluates to a well-established Laplace distirbution [5, 21, 41].

To characterize return trajectories, we start with the propagator for a particle in a harmonic potential:

$$G(x,x_0,t) = \sqrt{\frac{\mu K}{2\pi D(1 - e^{-2\mu Kt})}} \exp\left[-\frac{\mu K(x - x_0 e^{-\mu Kt})^2}{2D(1 - e^{-2\mu Kt})}\right],$$
(5)

which is the solution of $\dot{G}(x,x_0,t) = [\mu KxG(x,x_0,t)]' + DG''(x,x_0,t)$, subject to the initial condition $G(x,x_0,0) = \delta(x-x_0)$.

Like p(x,t), the propagator $G(x,x_0,t)$ does not capture the gradual disappearance of particles. In the return stage, particles vanish upon first arrival at the origin, which is implemented via an absorbing boundary at x = 0. We incorporate such an adsorbing walls using the method of images,

$$G_a(x,x_0,t) = G(x,x_0,t) - G(x,-x_0,t).$$

The propagator G_a is not normalized, and $S(t|x_0) = \int_0^\infty dx \, G_a(x,x_0,t)$ is the survival probability of a particle starting at x_0 .

Because return trajectories originate from positions distributed according to $n_{\text{off}}(x_0)$, the steady-state distribution is

$$n_{\rm on}(x) = \int_0^\infty dx_0 \, n_{\rm off}(x_0) \left[\frac{1}{\tau_{\rm on}} \int_0^\infty dt \, G_a(x, x_0, t) \right],$$
 (6)

where $\tau_{\rm on}$ is the mean return time (or $1/\tau_{\rm on}$ is the rate with which particles are adsorbed). Note that in the above expression we define $n_{\rm on}$ on the positive half-space $x \ge 0$, which is sufficient due to the even symmetry $n_{\rm on}(x) = n_{\rm on}(-x)$. The distribution in Eq. (6) is the solution of the following differential equation:

$$0 = [\mu K x n_{\rm on}]' + D n_{\rm on}'' + \frac{1}{\tau_{\rm on}} n_{\rm off}(x), \tag{7}$$

with absorbing boundary condition at x = 0. Evaluating Eq. (6) gives:

$$n_{\text{on}}(x) = \frac{1}{2} \sqrt{\frac{\pi}{2}} \sqrt{\frac{1}{D\tau_K}} \frac{\tau_K}{\tau_{\text{on}}} \exp\left[-\frac{1}{2} \frac{\tau_K}{\tau}\right] \exp\left[-\frac{1}{2} \frac{x^2}{D\tau_K}\right] \times \left[\operatorname{erfi}\left(\sqrt{\frac{1}{2} \frac{\tau_K}{\tau}}\right) - \operatorname{erfi}\left(\sqrt{\frac{1}{2} \frac{\tau_K}{\tau}} - \sqrt{\frac{1}{2} \frac{x^2}{D\tau_K}}\right) \right].$$
(8)

Here, $\tau_K = 1/(\mu K)$ is the relaxation time in the harmonic trap. Normalization $\int_0^\infty dx \, n_{\rm on}(x) = 1$ allows us to calculate $\tau_{\rm on}$,

$$\frac{\tau_{\rm on}}{\tau_K} = \frac{1}{2} e^{-\alpha/2} \left[\pi \operatorname{erfi} \sqrt{\frac{\alpha}{2}} - \operatorname{Ei} \left(\frac{\alpha}{2} \right) \right], \tag{9}$$

where we introduced a dimensionless rate at which outgoing trajectories are terminated,

$$\alpha = \frac{\tau_K}{\tau}$$
.

The result in Eq. (8) agrees with the derivation based on Fokker–Planck formalism in [26], confirming the accuracy of the integral equation formulation in Eq. (6) based on G_a .

Once τ_{on} is known, the fraction of particles in the "off" state becomes:

$$f = \frac{\tau}{\tau + \tau_{\rm on}},\tag{10}$$

and the full steady-state distribution reads:

$$n(x) = f n_{\text{off}}(x) + (1 - f) n_{\text{on}}(x).$$

Both $n_{\rm off}$ and $n_{\rm on}$ exhibit a cusp at x=0. The two cusps cancel each other when combined, producing a flat top in n(x), as seen in the left panels of Fig. (1). The probability of finding a particle in the "off" state is plotted in Fig. (2) as a function of a dimensionless rate of renewal $\alpha=\tau_K/\tau$. At a slow rate, $\alpha\to 0$, corresponding to long duration times of outgoing trajectories, f approaches 1 as most particles are found in the "off" state. Then, as the rate α increases, f slowly decays to zero as $f\sim \sqrt{2/\alpha\pi}$.

We note that the absorbing-boundary propagator of the OU process, $G_a(x,x_0,t)$, is restricted to the boundary at x=0. For an adsorbing boundary placed away from the origin, the source and image evolve with different velocities, producing a moving boundary. Attempts to correct this with a weight factor do not work, since such a factor is time-dependent, and the resulting image term would no longer solve the same Fokker–Planck equation. In those cases, one must resort to Laplace–transform or spectral–expansion techniques [42].

Finally, we draw attention to an interesting property of the distribution $\rho_{\rm on}=(1-f)n_{\rm on}$. While $\rho_{\rm on}$ is not normalized—the integral $\int_{-\infty}^{\infty} dx \, \rho_{\rm on}(x) = 1-f$ gives the probability of finding the particle in the "on" state— its second moment, when calculated in dimensionless coordinates $z=x/\sqrt{D\tau_K}$, is normalized:

$$\int_{-\infty}^{\infty} dz z^2 \, \rho_{\rm on}(z) = 1. \tag{11}$$

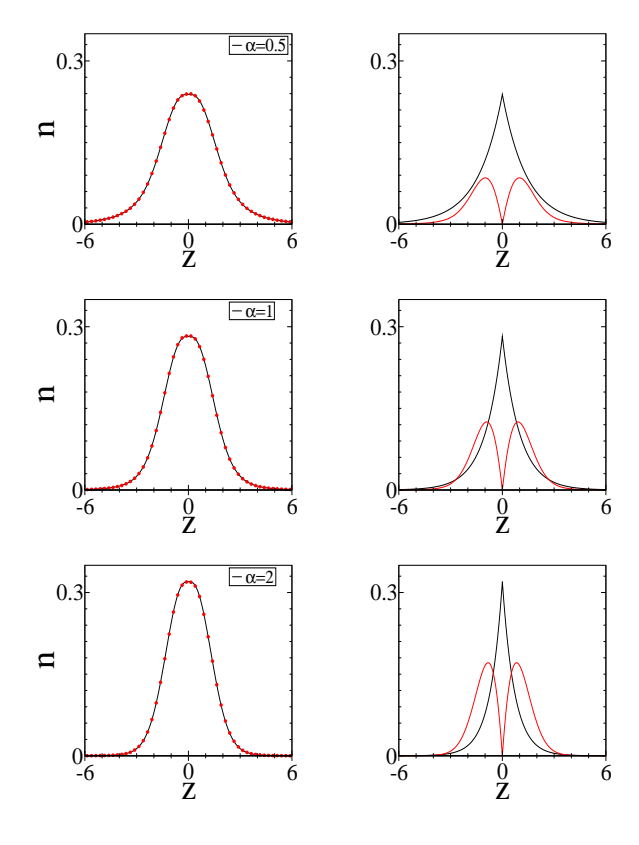


FIG. 1. Steady-state distributions as a function of dimensionless distance $z=x/\sqrt{D\tau_K}$ for various values of α . The left column shows the contributions from the two states: black lines correspond to the "off" state distribution $f n_{\rm off}$ as given in Eq. (4), and red lines correspond to the "on" state distribution $(1-f)n_{\rm on}$ given in Eq. (8). The right column shows the total normalized distribution $n=f n_{\rm off}+(1-f)n_{\rm on}$, where red circles denote simulation data, confirming analytical predictions.

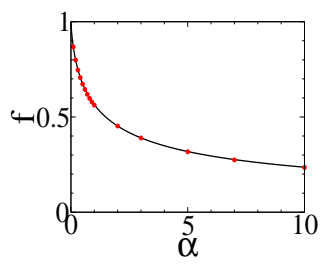


FIG. 2. Fraction of particles in the "off" state, f, as a function of $\alpha = \tau_K/\tau$, where $\tau_K = 1/(\mu K)$. Red circles are simulation results.

This identity can be directly verified by applying the operator $\int dx x^2$ to Eq. (7).

A direct implication is that the total average potential energy of the system is the same as that of a particle in thermal equilibrium:

$$PE = \int_{-\infty}^{\infty} dx \frac{Kx^2}{2} \rho_{\rm on}(x) = \frac{k_B T}{2}, \qquad (12)$$

Particles in the "off" state do not contribute to the potential

energy since the trap is turnd off during that phase.

This result holds for any r(t), provided the trap is harmonic. It is notable because it connects an equilibrium property to a non-equilibrium steady state.

B. waiting time distributions

Other quantities of interest are the waiting time distributions. Using the propagator $G_a(x,x_0,t)$, we define the survival function $S(t|x_0) = \int_0^\infty dx G_a(x,x_0,t)$, related to the first-passage-time distribution as $R_{\rm on} = -\dot{S}$, and leading to

$$R_{\rm on}(s|z_0) = e^{2s} \sqrt{\frac{z_0^2}{4\pi \left(e^s \sinh s\right)^3}} \exp\left(-\frac{z_0^2}{4e^s \sinh s}\right), \quad (13)$$

where we use the dimemnsionless variables of distance $z = x/\sqrt{D\tau_K}$ and time $u = t/\tau_K$, where $\tau_K = 1/(\mu K)$. $R_{\rm on}(s|z_0)$ represents the distribution of waiting times it takes a particle, initially at $z_0 = x_0/\sqrt{D\tau_K}$, to reach the origin for the first time.

From $R_{on}(s|z_0)$ we calculate the mean time,

$$\langle s \rangle_{z_0} = \int_0^\infty ds \, s \, R_{\rm on}(s|z_0),$$

which, after evaluation, becomes

$$\langle s \rangle_{z_0} = \frac{1}{2} \left[\pi \operatorname{erfi}\left(\frac{z_0}{\sqrt{2}}\right) - z_{02}^2 F_2\left(1, 1; \frac{3}{2}, 2; \frac{z_0^2}{2}\right) \right].$$
 (14)

Since this quantity will be frequently used in defining the mean first passage time of various protocols, below we provide an explicit expression in physical parameters,

$$t_{\text{on}}(x_0) = \frac{\tau_K}{2} \left[\pi \operatorname{erfi} \sqrt{\frac{x_0^2}{2D\tau_K}} - \frac{x_0^2}{D\tau_K} {}_2F_2\left(1, 1; \frac{3}{2}, 2; \frac{x_0^2}{2D\tau_K}\right) \right],$$
(15)

where $t_{\rm on}$ is related to $\langle s \rangle_{z_0}$ via $t_{\rm on} = \langle s \rangle_{z_0} \tau_K$. The above expression represents the mean time to reach x = 0 for the first time for a particle in a harmonic trap and initially at x_0 .

The waiting time distribution that a particle remains in the "on" state, designated by $r_{on}(u)$, is obtained by averaging R_{on} over the distribution of initial positions:

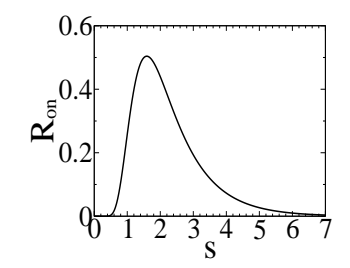
$$r_{\rm on}(u) = \int_{-\infty}^{\infty} dz_0 \, n_{\rm off}(z_0) R_{\rm on}(s|z_0).$$
 (16)

Inserting $n_{\text{off}}(z)$ and $R_{\text{on}}(s|z_0)$ into Eq. (16) yields

$$r_{\rm on}(u) = \alpha e^{2s} \left[\frac{1}{\sqrt{\pi \alpha e^s \sinh s}} - e^{\alpha e^s \sinh s} \operatorname{erfc} \left(\sqrt{\alpha e^s \sinh s} \right) \right], \tag{17}$$

where $\alpha = \tau_K/\tau$.

In Fig. (3) we plot the first-passage-time distributions $R_{\text{on}}(s|z_0)$ and $r_{\text{on}}(u)$. Although r_{on} is derived from R_{on} , their behaviors at short times differ drastically.



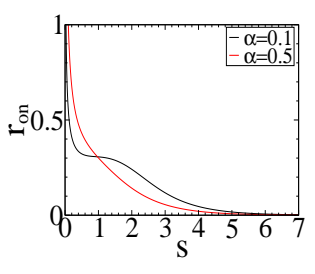


FIG. 3. First-passage-time distributions as a function of dimensionless time $u = t/\tau_K$. The left panel shows $R_{\rm on}(s|z_0)$ for a particle initially located at $z_0 = 5$, while the right panel displays the total return-time distribution $r_{\rm on}(u)$ for different values of α . The exact expressions are given in Eq. (13) for $R_{\rm on}(s,z_0)$ and in Eq. (17) for $r_{\rm on}(u)$.

These features are evident from the respective asymptotic behaviors:

$$R_{\rm on}(s,z_0) \sim \begin{cases} \frac{e^{-z_0^2/4s}}{\sqrt{4\pi s^3}} z_0 e^{z_0^2/4}, & \text{as } s \to 0, \\ e^{-s} z_0 \sqrt{\frac{2}{\pi}}, & \text{as } s \to \infty, \end{cases}$$
(18)

and

$$r_{\rm on}(u) \sim \begin{cases} \sqrt{\frac{\alpha}{\pi s}}, & \text{as } s \to 0, \\ e^{-s} \sqrt{\frac{2}{\alpha \pi}}, & \text{as } s \to \infty. \end{cases}$$

While both functions exhibit exponential decay at large s, only $r_{\rm on}(u)$ diverges for small s. This divergence originates from the structure of the distribution $n_{\rm off}$, which allows initial positions arbitrarily close to $z_0=0$, yielding return times near zero.

C. Time-Energy Trade-Off

In this section, we briefly look at the energy consumption of return trajectories due to the external driving force.

The class of models in which return trajectories are terminated at random times drawn from a prescribed distribution $r_{\rm on}(t)$ —in contrast to our protocol, where $r_{\rm on}(t)$ emerges self-consistently—has two main drawbacks. First, the outgoing trajectories originate from a broad distribution of initial positions rather than from the fixed point x=0. Second, the randomly sampled return times are often too short for this distribution to relax to equilibrium; consequently, the initial-position distribution is not Gaussian but dominated by exponential tails extending far from the origin.

One can partially correct this issue by allowing the return trajectories sufficient time to equilibrate, so that $n_{\rm on}$ approaches a Boltzmann distribution, $n_{\rm on} \propto e^{-x^2/2D\tau_K}$ [25]. Although this does not ensure that the outgoing trajectories start exactly from x=0, it provides a substantial improvement

over a distribution that has an exponential tail. From Eq. (5), we know that the mean position of a particle in a harmonic trap decays as $\langle x(t) \rangle = x_0 e^{-t/\tau_K}$. A common rule of thumb based on this result is that equilibration is effectively reached at $\tau_{\rm eq} \approx 3\tau_K$.

To see how $\tau_{\rm on}$ of our model compares with $\tau_{\rm eq}$, in Fig. (4) we plot $\tau_{\rm on}$ as a function of τ , We observe that $\tau_{\rm on}$ remains below $\tau_{\rm eq}$, except for very large values of τ , approximately $\tau \gtrsim 300\,\tau_K$. Thus, our protocol, in addition to ensuring the precise starting point of outgoing trajectories, is faster compared to passive equilibration.

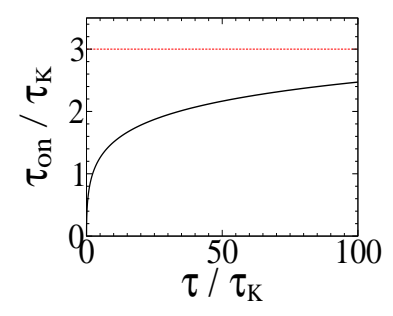


FIG. 4. Mean return time $\tau_{\rm on}$ as a function of τ . The dashed line marks the passive equilibration time $\tau_{\rm eq} \approx 3 \tau_{\rm K}$. $\tau_{\rm on}$ remains below $\tau_{\rm eq}$ except for very large ratios $\tau/\tau_{\rm K}$.

To understand the behavior of τ_{on} at large τ/τ_K (corresponding to large K), we examine its asymptotic form in the limit of large K:

$$\frac{\tau_{\rm on}}{\tau_K} \sim \frac{1}{2} \ln \frac{\tau}{\tau_K}.\tag{19}$$

The fact that $\tau_{\rm on}$ eventually exceeds $\tau_{\rm eq}$ follows from the logarithmic factor in Eq. (19), which is a hallmark of first-passage in a harmonic trap. Its origin can be traced to the mean first-passage time conditioned on the initial offset $z_0 = x_0/\sqrt{D\tau_K}$:

$$\langle s \rangle_{z_0} = \int_0^\infty s \, R_{\text{on}}(s \, | \, z_0) \, ds \sim \ln z_0 + \frac{1}{2} \left(\gamma + \ln 2 \right), \qquad (z_0 \gg 1).$$

so that averaging $\langle s \rangle_{z_0}$ over the initial-position distribution $n_{\rm off}(x_0)$ produces the overall logarithm in Eq. (19). The absence of a logarithmic term in $\tau_{\rm eq}$ has more to do with the convention $\tau_{\rm eq} \approx 3\,\tau_K$. A more accurate definition of $\tau_{\rm eq}$ would likely yield a similar logarithmic factor. However, we will not pursue refinements of the definition of $\tau_{\rm eq}$ in this work and use $\tau_{\rm eq} \approx 3\,\tau_K$ as sufficient for what we wish to demonstrate.

We next turn to the question of energy. The parameter K gives us control over how fast the return process is complete. By increasing K, $\tau_{\rm on}$ can be reduced to an arbitrarily low value. The key question, however, is: at what energetic cost?

The instantaneous energy of a particle when the trap is switched on is $u = \frac{1}{2}Kx_0^2$, where x_0 is the initial position of the return trajectory. The trajectory terminates when the particle reaches the origin, at which point this energy has been entirely dissipated as heat. Averaging over the distribution of

initial positions $n_{\text{off}}(x_0)$ (see Eq. 16), the mean dissipated energy per cycle is

$$\Delta E = \int_{-\infty}^{\infty} dx_0 \, n_{\text{off}}(x_0) \, u(x_0) = DK\tau. \tag{20}$$

We now compare this result with the energy balance for particles equilibrating inside a harmonic potential. Since outgoing trajectories in this case start from a Boltzmann distribution, the particles are more spatially spread at the moment the trap is switched on. The mean potential energy at that instant is $\langle u(x_0)\rangle_1=DK\left(\tau+\frac{\tau_K}{2}\right)$, where the second term accounts for the fact that particles do not start from the origin but from an equilibrium distribution. At the end of equilibration, when the potential is switched off, the equilibrium mean energy is $\langle u(x_0)\rangle_2=DK\frac{\tau_K}{2}$. Taking the difference, $\Delta E=\langle u(x_0)\rangle_1-\langle u(x_0)\rangle_2$, recovers the result in Eq. (20). Hence, our first-passage-based protocol dissipates the same amount of heat as the protocol based on full equilibration. The advantage is that our protocol does it more precisely, by bringing particles to the origin, and doing it faster.

The above analysis suggests a speedup relative to passive equilibration without any additional mechanical energy cost. It is important to mention another protocol, the Engineered Swift Equilibration (ESE) scheme proposed in [25, 43]. In ESE, the system is driven to equilibrium within a prescribed time by engineering a time-dependent potential K(t). While ESE achieves fast equilibration, it necessarily incurs a higher energetic cost. In contrast, our protocol attains a comparable speedup without mechanical energy penalties.

While ESE accelerates relaxation by injecting energy, our protocol uses *information* to accelerate the return phase. This places our model in the broader class of Maxwell-demon systems such as the information ratchet [44, 45] or the Szilard's engine [46].

1. entropy production

Having determined the amount of energy injected during a single cycle, the steady-state rate of heat dissipation, \dot{q} , can be obtained by dividing ΔE by the mean duration of a cycle, $\tau + \tau_{\rm on}$. Using the standard thermodynamic relation $\dot{q} = T\Pi$, where Π is the entropy production rate and T is the temperature, we find:

$$T\Pi = \dot{q} = \frac{\Delta E}{\tau + \tau_{\rm on}} = DK \left(\frac{\tau}{\tau + \tau_{\rm on}}\right) = DKf,$$
 (21)

where f denotes the fraction of particles in the "off" state under steady-state conditions. Somewhat counterintuitively, Π increases as the particle spends more time in the "off" state.

The entropy production of stochastic resetting processes in arbitrary external potentials has been analyzed from a formal perspective in Ref. [47]. Our derivation is more intuitive and for a specific system. Other formal studies related to the entropy production rate or other non-equilibrium aspects of stochastic resetting can be found in [48–50].

III. THE MEAN FIRST PASSAGE TIME

An important feature of the SR protocols is their ability to optimize search efficiency by eliminating unproductive trajectories. Rather than allowing a particle to wander indefinitely when the target is not found, the system resets: the particle is returned to its initial position, and a new search begins. This interruption mechanism is key to improving the mean time to locate a target.

In this section, we analyze four distinct SR protocols. The difference between them lies in how the return trajectories are used. These protocols are:

- SR: The basic resetting protocol, with outgoing trajectories and without return trajectories.
- **SR-A:** A protocol that includes a reverse trajectory; however, the trajectory is *invisible* to the target, so the target cannot be located during a return motion.
- **SR-B:** Similar to SR-A, but with a *visible* return trajectory. As a result, the target can be located by the return trajectory.
- **SR-C:** A protocol involving only return trajectories. As soon as the particle reaches x = 0, it is instantly transferred to a new starting point $x_0 \neq 0$, and the next return trajectory is initiated.

Our approach to computing the MFPT is based on decomposing the full resetting process into generations of trajectories and then decomposing each process within each generation into phenomenological parameters and characteristic timescales. Since the target is located at x = L, and the return termination occurs at x = 0, the process is naturally framed as a two-boundary problem. These two absorbing boundaries give rise to a splitting probability scenario. Each parameter is then defined and computed within this framework.

The idea of using return trajectories as an active part of the search process has recently been explored in [33, 34]. Our approach differs both in derivation and in scope. Rather than analyzing a single protocol, we construct and compare several search protocols based on the same potential landscape. Furthermore, our proposal of the SR-C protocol introduces a novel perspective: a search mechanism that relies solely on return motion, bypassing the traditional outward exploration phase altogether.

A. definitions and notation

In this section we collect the parameters and distributions defined in the previous section. These quantities will be used to derive the MFPT for the various protocols discussed later in the paper.

Time scales:

au — average duration of an outgoing trajectory, corresponding to the exponential distribution $r(t)= au^{-1}e^{-t/ au}$.

 $\tau_K = 1/(\mu K)$ — Ornstein–Uhlenbeck relaxation time of a harmonic trap of stiffness K.

 $\tau_{\rm on}$ — average duration of a return trajectory drawn from the distribution $r_{\rm on}(t)$ and defined as

$$\frac{\tau_{\rm on}}{\tau_{\rm K}} = \frac{1}{2} e^{-\alpha/2} \left[\pi \operatorname{erfi} \sqrt{\frac{\alpha}{2}} - \operatorname{Ei} \left(\frac{\alpha}{2} \right) \right], \tag{22}$$

where $\alpha = \tau_K/\tau$.

 $t_{\rm on}(x_0)$ — the mean first passage time of a particle in a harmonic trap initially in x_0 , defined as

$$t_{\text{on}}(x_0) = \frac{\tau_K}{2} \left[\pi \operatorname{erfi} \sqrt{\frac{x_0^2}{2D\tau_K}} - \frac{x_0^2}{D\tau_K} {}_2F_2\left(1, 1; \frac{3}{2}, 2; \frac{x_0^2}{2D\tau_K}\right) \right].$$
(23)

The search process is partitioned into identical cycles, each composed of an outgoing trajectory (starting at x=0) and a return trajectory (ending at x=0). A particle may find the target during either stage. Table I summarizes the quantities used in defining the mean first passage time (MFPT).

p Probability that an outgoing trajectory is successful

1-p Probability that an outgoing trajectory is unsuccessful

q Probability that a return trajectory is successful

1-q Probability that a return trajectory is unsuccessful

 τ_p Mean duration of a successful outgoing trajectory

 τ_{1-n} Mean duration of an unsuccessful outgoing trajectory

 au_q Mean duration of a successful return trajectory

 τ_{1-q} Mean duration of an unsuccessful return trajectory

TABLE I. Quantities characterizing the outgoing and return stages of each search cycle.

B. SR protocol

We start with the basic SR protocol, which does not include return trajectories, and the moment that an outgoing trajectory is interrupted a particle appears at x = 0. We revisit this protocol to introduce our approach for calculating the mean first-passage time (MFPT).

Due to the cyclical nature of the SR protocol, it is useful to organize trajectories into *generations*. Trajectories that have never been renewed are called *first generation*; those renewed once are *second generation*; and so on. The probability of finding a target by any single trajectory is 0 and, therefore, the probability of missing a target is <math>1 - p.

If a targe is not found duing a first generation, it may be found at second, third, etc. The probability that a target is found after n attempts is defined as

$$p_n = (1 - p)^{n-1} p, (24)$$

indicating that the last successful trajectory was preceded by n-1 unsuccessful trajectories. Summing over all possible generations, we get

$$\sum_{n=1}^{\infty} p_n = 1,\tag{25}$$

which shows that the protocol always finds the target as long as 0 .

Next, we compute the mean time for a sequence of n trajectories to find the target. Let τ_p denote the mean time of a single successful trajectory, and τ_{1-p} the mean time of a single unsuccessful trajectory. Note that $\tau_{1-p} \neq \tau$ since it accounts only for unsuccessful trajectories. Considering that a target is found after n attempts, the mean time due to all the n outgoing trajectories is given by

$$\tau_n = (n-1)\,\tau_{1-p} + \tau_p,\tag{26}$$

where the (n-1) unsuccessful trajectories each contribute τ_{1-p} and the final successful trajectory contributes τ_p .

Having defined p_n and τ_n , the MFPT of the entire SR protocol can be written as

$$\tau_{\rm sr} = \sum_{n=1}^{\infty} p_n \, \tau_n,\tag{27}$$

which evaluates to

$$\tau_{\rm sr} = \tau_p + \frac{1-p}{p} \, \tau_{1-p},$$
(28)

which shows that $\tau_{\rm sr} \geq \tau_p$, which makes sense since on average the target is not found at a first attempt.

Defining the average number of generations required to find the target as $\langle n \rangle = \sum_{n=1}^{\infty} n p_n = p^{-1}$, the MFPT can be expressed as

$$\tau_{\rm sr} = \langle n \rangle \left[p \, \tau_p + (1 - p) \, \tau_{1-p} \right]. \tag{29}$$

Thus, the MFPT of the SR protocol is proportional to the average number of generations required to find a target multiplied by a weighted average of the two characteristic time scales.

1. derivation of the MFPT expression

The MFPT for the SR-A protocol in Eq. (28) is defined in terms of three parameters: p, τ_{1-p} , and τ_p . We next show how these parameters emerge from underlying dynamics.

We start by defining the distribution of first-passage times for trajectories without stochastic interruptions, h(t), which by being normalized, $\int_0^\infty dt \, h(t) = 1$, implies that eventually all trajectories find a target. The second distribution needed is the distirbution of times a particle remains in an outgoing stage, r(t), which for our particular model is an exponential distribution

Associated with both distributions r(t) and h(t) are the corresponding survival functions,

$$S_r(t) = \int_t^\infty dt' \, r(t'), \qquad S_h(t) = \int_t^\infty dt' \, h(t'). \tag{30}$$

The probability p of a successful trajectory and the corresponding mean time τ_p can then be defined in terms of those quantities as

$$p = \int_0^\infty dt \, h(t) \, S_r(t),$$

$$p \, \tau_p = \int_0^\infty dt \, t \, h(t) \, S_r(t). \tag{31}$$

Analogously, we can write

$$1 - p = \int_0^\infty dt \, r(t) \, S_h(t),$$

$$(1 - p) \, \tau_{1-p} = \int_0^\infty dt \, t \, r(t) \, S_h(t). \tag{32}$$

For exponential r(t), the survival function satisfies $S_r(t) = \tau r(t)$, and $S_r(t) = -\tau^2 \dot{r}(t)$. Using these relations, the second equation in ((32)) yields

$$(1-p)\,\tau_{1-p} + p\,\tau_p = (1-p)\,\tau,\tag{33}$$

which allows us to rewrite Eq. (28) for the MFPT as

$$\tau_{\rm sr} = \frac{1-p}{p} \, \tau. \tag{34}$$

Thus, the expression of τ_{sr} for the SR protocol involves two parameters $\{p, \tau\}$.

For the targer located at x=L, the parameter p can be calculated from the first integral in Eq. (31), given that h(t) is represented by the inverse Gaussian distribution, $h(t) = \sqrt{L^2/4\pi Dt^3}e^{-L^2/4Dt}$, leading to

$$p = e^{-L/\sqrt{D\tau}}. (35)$$

C. SR-A protocol

As the first extension of the SR protocol, we consider the protocol with "invisible" return trajectories. The only contribution of these trajectories is to increase the duration of a single cycle, which in turn increases the resulting MFPT.

Because return trajectories are invisible to the target, the probability of a single return trajectory to find a target is q = 0, and the probability of an unsuccessful return trajectory is 1 - q = 1. Finally, the mean time of an unsuccessful return trajectory is designated by τ_{1-q} .

If a target is found after n attempts, the mean time of that sequence of attempts is given by

$$\tau_n = (n-1)(\tau_{1-p} + \tau_{1-q}) + \tau_p, \tag{36}$$

where τ_p is due to the last successful attempt, and $(n-1)(\tau_{1-p}+\tau_{1-q})$ is due to n-1 unsuccessful attempts which include contributions of an unsuccessful outgoing and return trajectory. The result in Eq. (36) together with p_n defined in Eq. (24), the formula for τ_{sr} in Eq. (27) yields

$$\tau_{\rm sr} = \tau_p + \frac{1 - p}{p} (\tau_{1-p} + \tau_{1-q}). \tag{37}$$

And since $\langle n \rangle = p^{-1}$, this expression can be written as

$$\tau_{\rm sr} = \langle n \rangle \left[p \tau_p + (1 - p)(\tau_{1-p} + \tau_{1-q}) \right], \tag{38}$$

indicating that the MFPT is equal to the average number of generations, $\langle n \rangle$, multiplied by a weighted combination of characteristic times — the mean duration of a successful trajectory, τ_p , and the total mean time associated with a failed attempt, $\tau_{1-p} + \tau_{1-q}$.

For the exponential distribution r(t), we can use the relation in Eq. (33), which modifies the formula in Eq. (36) to

$$\tau_{sr} = \frac{1-p}{p} \left(\tau + \tau_{1-q} \right). \tag{39}$$

1. derivation of the MFPT expression

The only parameter not previously defined is τ_{1-q} , representing the mean time of an unsuccessful trajectory to reach the origin. To calculate τ_{1-q} , we need the mean first passage time to x=0 from an initial point x_0 , designated by $t_{\rm on}(x_0)$ and defined in Eq. (23). In addition, we need the distribution of initial positions x_0 , which is different from $n_{\rm off}$, due to the absorbing boundary conditions at the location of a target x=L, to account for absence of successful trajectories. We represent such a distribution using the image method involving two Laplace distributions as

$$n_L(x_0) = A \left[e^{-|x_0|/\sqrt{D\tau}} - e^{-|x_0 - 2L|/\sqrt{D\tau}} \right],$$
 (40)

where A is a normalization constant such that $\int_{-\infty}^{L} dx_0 \, n_L(x_0) = 1$. The time τ_{1-q} can now be represented as

$$\tau_{1-q} = \int_{-\infty}^{L} dx_0 n_L(x_0) t_{\text{on}}(x_0). \tag{41}$$

Together with Eq. (39), this expression fully determines the MFPT for the SR-A protocol. In this protocol, the presence of an "invisible" return trajectory extends the MFPT. The MFPT expression involves three parameters $\{p, \tau, \tau_{1-q}\}$.

D. SR-B protocol

In this section we consider a protocol in which return trajectories are allowed to participate in a target search. The probability of finding a target by a single return trajectory in this protocol is q > 0.

The probability of finding a target by an outgoing trajectory on a *n*-th attempt is given by

$$p_n = [(1-p)(1-q)]^{n-1} p. (42)$$

Prior to a n-th successful outgoing trajectory, there were n-1 unsuccessful outgoing and returning trajectories. Setting q=0 recovers the SR-A case from Eq. (24).

Similarly, the probability of finding a target by a returning trajectory on a *n*-th attempt is

$$q_n = [(1-p)(1-q)]^{n-1}(1-p)q. \tag{43}$$

Prior to the successful n-th return trajectory, there are n unsuccessful outgoing trajectories and n-1 unsuccessful return trajectories.

We can verify that the total probability of locating the target — whether during an outgoing or a return trajectory — is properly normalized:

$$\sum_{n=1}^{\infty} (p_n + q_n) = 1.$$

We next define the mean time of finding a target for a sequence of n trajectories, considering that a target is found by an outgoing trajectory,

$$\tau_n^{\text{out}} = (n-1)(\tau_{1-p} + \tau_{1-q}) + \tau_p. \tag{44}$$

The expression is similar to that in Eq. (36). The difference lies in that τ_{1-q} is defined differently due to the exclusion of return trajectories that find a target.

An expression for the mean time of finding a target by a sequence of n trajectories, assuming that the target is located by a return trajectory, is given by

$$\tau_n^{\text{ret}} = (n-1)\tau_{1-q} + n\tau_{1-p} + \tau_q, \tag{45}$$

where τ_q is the mean time of finding a target by a single return trajectory.

Having defined p_n , q_n , τ_n^{out} , and τ_n^{ret} , the MFPT of the entire SR-B process, defined as

$$au_{
m sr} = \sum_{n=1}^{\infty} \left(p_n au_n^{
m out} + q_n au_n^{
m ret}
ight),$$

yields

$$\tau_{\rm sr} = \frac{p\tau_p + (1-p)\tau_{1-p} + (1-p)q\tau_q + (1-p)(1-q)\tau_{1-q}}{p+q-pq}.$$
(46)

For an exponential r(t) we can use Eq. (33) Which reduces the above formula to

$$\tau_{\rm sr} = \frac{(1-p)\tau + (1-p)(1-q)\tau_{1-q} + q(1-p)\tau_q}{p+q-pq}.$$
 (47)

The MFPT of the SR-B protocol therefore depends on five parameters, $\{p,q,\tau,\tau_{1-q},\tau_q\}$. Three of these parameters, $\{q,\tau_{1-q},\tau_q\}$, need to be defined. τ_{1-q} of the SR-A protocol is not the same as τ_{1-q} of the current SR-B protocol.

1. derivation of the MFPT expression

To define these parameters, we first need to describe the physical scenario underlying the SR-B protocol. Because the presence of the target x=L and the off-switch at x=0 can be represented as two adsorbing walls, the situation corresponds to a random walker enclosed by two adsorbing walls at x=0 and x=L. This gives rise to the splitting probability setup, therefore, the missing parameters can be defined within that framework.

For a particle in a harmonic potential, initially at $x_0 \in (0, L)$, the splitting probability $\pi_L(x_0)$ — that is, the probability of reaching x = L before x = 0 — is known to satisfy the following backward Fokker–Planck equation [51]:

$$0 = \mu K x_0 \, \pi'_L(x_0) - D \, \pi''_L(x_0),$$

subject to the boundary conditions $\pi_L(0) = 0$ and $\pi_L(L) = 1$. The solution is:

$$\pi_L(x_0) = \frac{\int_0^{x_0} dx \, e^{\mu K x^2 / (2D)}}{\int_0^L dx \, e^{\mu K x^2 / (2D)}}.$$
 (48)

To compute q, the probability of locating a target by a single return trajectory, we must consider the distribution of initial points x_0 , which are distributed according to $n_L(x_0)$, already defined in Eq. (40). This yields

$$q = \int_0^L dx_0 n_L(x_0) \pi_L(x_0). \tag{49}$$

To determine τ_q , the mean duration of a single successful return trajectory, we consider the mean first passage time for a particle starting at x_0 to reach x = L without first being absorbed at x = 0. This quantity, designated by $t_L(x_0)$, satisfies the following backward differential equation:

$$\pi_L(x_0) = \mu K x_0 t'_L(x_0) - D t''_L(x_0),$$

with boundary conditions $t_L(0) = t_L(L) = 0$. The solution is given by

$$t_L(x_0) = \frac{1}{D} \int_0^{x_0} dx \, e^{\mu K x^2 / 2D} \int_x^L dx' \, e^{-\mu K x'^2 / 2D} \pi_L(x')$$
$$- \frac{\pi_L(x_0)}{D} \int_0^L dx \, e^{\mu K x^2 / 2D} \int_x^L dx' \, e^{-\mu K x'^2 / 2D} \pi_L(x').$$

The quantity τ_q is then obtained by considering a distribution of initial points x_0 ,

$$q\tau_q = \int_0^L dx_0 \, n_L(x_0) t_L(x_0). \tag{50}$$

Finally, to define τ_{1-q} , the mean duration of a single unsuccessful return trajectory, which is differently defined from τ_{1-q} in Eq. (41), we consider the mean first passage time for a particle starting at x_0 to reach x=0 without first being absorbed at x=L. This quantity, designated by $t_0(x_0)$, satisfies the following differential equation

$$\pi_0(x_0) = \mu K x_0 t_0'(x_0) - D t_0''(x_0), \tag{51}$$

where $\pi_0(x_0) = 1 - \pi_L(x_0)$ is the splitting probability to reach x = 0 before x = L. The solution is

$$t_0(x_0) = \frac{1}{D} \int_{x_0}^{L} dx \, e^{\mu K x^2 / (2D)} \int_{0}^{x} dx' \, e^{-\mu K x'^2 / (2D)} \pi_0(x')$$
$$- \frac{\pi_0(x_0)}{D} \int_{0}^{L} dx \, e^{\mu K x^2 / (2D)} \int_{0}^{x} dx' \, e^{-\mu K x'^2 / (2D)} \pi_0(x'). \tag{52}$$

The quantity τ_{1-q} is then obtained from the relation

$$(1-q)\tau_{1-q} = \int_0^L dx_0 \, n_L(x_0)t_0(x_0) + \int_{-\infty}^0 dx_0 \, n_L(x_0)t_{\text{on}}(x_0),$$
(53)

where the second integral accounts for the initial positions $x_0 < 0$ that are prevented from reaching the target at x = L due to the adsorbing wall at x = 0. We recall that t_{on} is defined in Eq. (23).

2. results

Having defined all the parameters, we are ready to calculate the MFPT. Fig. (5) compares the MFPTs for the SR-A and SR-B protocols, given by Eqs. (39) and (47), with the data points from numerical simulations. The close agreement across the explored parameter range confirms the correctness of the analytical formulas.

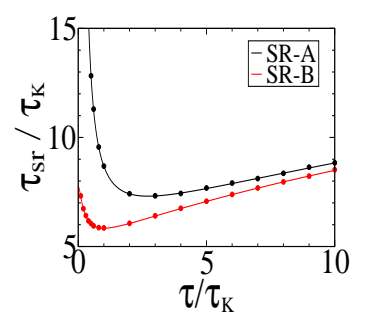


FIG. 5. MFPT as a function of τ for the SR-A and SR-B protocols, corresponding to Eq. (39) and Eq. (47), compared with the simulation data points. The results are for $b = 1/\sqrt{0.3}$, where $b = L/\sqrt{D\tau_K}$.

Since both SR-A and SR-B protocols include return trajectories, their MFPTs are expected to be greater than that of the SR protocol. And since in SR-B the return trajectories contribute to the search, the overhead time associated with the return motion is reduced. Consequently, we anticipate the following relation: $\tau_{\text{sr}}^{\text{SR}} \leq \tau_{\text{sr}}^{\text{SR-B}} \leq \tau_{\text{sr}}^{\text{SR-A}}.$ In Fig. 6, we plot the MFPT as a function of τ for the

In Fig. 6, we plot the MFPT as a function of τ for the three protocols analyzed above. Note that the relation $\tau_{\rm sr}^{\rm SR} \leq \tau_{\rm sr}^{\rm SR-A} \leq \tau_{\rm sr}^{\rm SR-A}$ is satisfied most of the time, except in the region of small τ , where SR-B becomes the fastest protocol. It is also the only protocol whose MFPT does not diverge in the limit $\tau \to 0$. This suggests that reverse search under certain conditions becomes more efficient than the forward search.

To understand this situation, we need to clarify why the MFPT diverges for the SR and SR-A protocols as $\tau \to 0$. In these protocols, the outgoing trajectories become too shortlived to reach the target. As a result, the number of generations required for a successful hit diverges.

In the $\tau \to 0$ limit, outgoing trajectories are effectively suppressed. This implies that only return trajectories can contribute to locating the target. However, for SR and SR-A, return trajectories are either absent or invisible to the target. Only the SR-B protocol can use these return trajectories productively in the search.

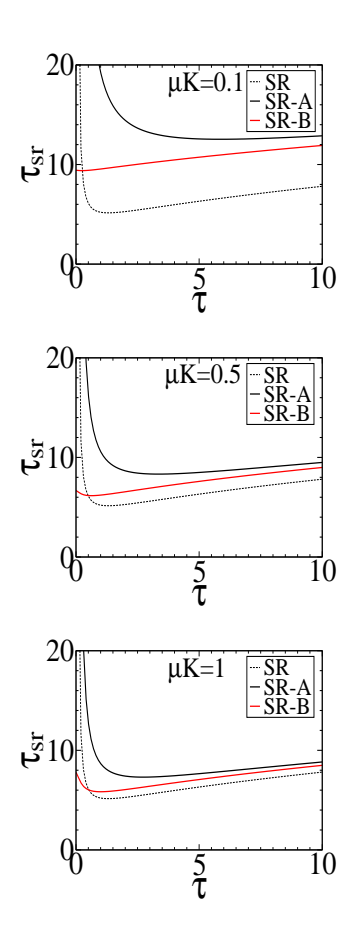


FIG. 6. MFPT as a function of τ for three types of the SR protocol and for three values of the stiffness parameter, K. The results in this figure are for L=1 and D=0.3.

Given the vanishing duration of the "off" state in the limit $\tau \to 0$, the harmonic trap is effectively permanent, and the initial position of each return trajectory approaches the origin. The problem reduces to computing the MFPT for a particle starting at x=0 in a harmonic potential, searching for a target located at x=L. The MFPT for this problem is well known [51, 52] and given by:

$$\tau_{sr}^{0} = \frac{1}{D} \int_{0}^{L} dx \, e^{\mu K x^{2}/2D} \int_{-\infty}^{x} dx' \, e^{-\mu K x'^{2}/2D}, \qquad (54)$$

which evaluates to

$$\tau_{\rm sr}^0 = \frac{\tau_K}{2} \left[\pi \operatorname{erfi} \sqrt{\frac{b^2}{2}} + b^2 {}_2F_2\left(1, 1; \frac{3}{2}, 2; \frac{b^2}{2}\right) \right], \quad (55)$$

where $b = L/\sqrt{D\tau_K}$, and $_2F_2$ denote generalized hypergeometric functions.

This expression, though finite, is not bounded in b; it grows with distance to the target. But critically, it demonstrates that the MFPT for SR-B remains finite as $\tau \to 0$, unlike the diverging behavior of SR and SR-A.

We conclude that the enhanced efficiency of SR-B in the $\tau \to 0$ regime stems not from the intrinsic advantage of reverse search, but from the fact that it remains operative when

outgoing trajectories are suppressed. It reduces to the first passage problem of a particle in a permanent trap. This behavior has been observed in [33, 34], which primarily focused on a linear potential.

E. SR-C: protocol without the outgoing trajectories

In this section, we introduce a protocol that entirely eliminates outgoing trajectories: the search is performed solely via return paths. In this scenario, a particle begins its motion from a position sampled from the distribution $n_{\rm off}(x_0)$, given in Eq. (4), and is then driven by a harmonic force toward the origin. If the particle reaches the origin without locating the target, it is instantaneously relocated to a new starting position, again drawn from $n_{\rm off}$. This instantaneous (and unphysical) reset resembles the standard SR protocol, but with a critical distinction.

Unlike traditional SR, the present model incorporates an additional control parameter—the strength of the restoring force—that allows us to modulate the efficiency of the search. Furthermore, the driven return motion bears similarities to active motion. However, in contrast to active motion, where directionality is stochastic, here the motion is persistently oriented toward the origin.

1. time-dependent distribution

Since the idea of stochastic resetting suggested by the SR-C protocol is novel, in this section we analyze its time-dependent distribution, $n_{\text{on}}(x,t)$, which satisfies the partial differential equation:

$$\dot{n}_{\rm on} = \left[\mu K x n_{\rm on}\right]' + D n_{\rm on}'' + j(t) n_{\rm off}(x),\tag{56}$$

with boundary condition $n_{\rm on}(0,t)=0$, and initial condition $n_{\rm on}(x,0)=n_{\rm off}(x)$. The flux at the absorbing boundary is defined by

$$j(t) = D \partial_x n_{\text{on}}(x, t) \Big|_{x=0}. \tag{57}$$

We consider only the distribution in the half-line $x \ge 0$, which is sufficient due to the even symmetry: $n_{\text{on}}(x,t) = n_{\text{on}}(-x,t)$.

The solution in the positive half-space admits the renewal form:

$$n_{\text{on}}(x,t) = \int_{0}^{\infty} dx' G_{a}(x,x',t) n_{\text{off}}(x') + \int_{0}^{t} dt' j(t') \int_{0}^{\infty} dx' G_{a}(x,x',t-t') n_{\text{off}}(x').$$
 (58)

The first term describes evolution of the initial state, while the second accounts for successive reinjections at the origin.

The flux function j(t) satisfies another renewal equation [53–55],

$$j(t) = r_{\rm on}(t) + \int_0^t dt' \, j(t') \, r_{\rm on}(t - t'), \tag{59}$$

which captures the recursive structure of returns. At short times, $j(t) \approx r_{\rm on}(t)$, while at long times the flux approaches its steady-state value:

$$j(t) \rightarrow \tau_{\rm on}^{-1}$$
.

It can be verified that the distribution is conserved at all times,

$$\int_{0}^{\infty} dx \, n_{\rm on}(x,t) = \frac{1}{2}.\tag{60}$$

As $t \to \infty$, the distribution $n_{\rm on}(x,t)$ approaches the stationary form given by Eq. (6).

2. MFPT

Based on previous expressions of τ_{sr} derived for other protocols, the MFPT of the SR-C protocol is found to be defined analogously to Eq. (28):

$$\tau_{sr} = \frac{q \,\tau_q + (1 - q) \,\tau_{1 - p}}{q},\tag{61}$$

where q is the probability that a single (return) trajectory finds the target, τ_q is the mean duration of a single successful trajectory, and τ_{1-p} is the mean duration of a single unsuccessful trajectory (one that reaches x=0 without finding the target). Thus, the MFPT depends on three parameters, $\{q, \tau_q, \tau_{1-p}\}$, which we will define below.

3. derivation of the MFPT expression

We define the probability for a single trajectory to find the target as

$$q = \int_{L}^{\infty} dx_0 \, n_{\text{off}}(x_0) + \int_{0}^{L} dx_0 \, n_{\text{off}}(x_0) \pi_L(x_0). \tag{62}$$

The first term of the expression captures contributions of all the trajectories with the initial position $x_0 \ge L$. All these trajectories find the target en route to x=0, assuming that K>0. The second term represents the contributions of the trajectories with the initial position in the interval $x_0 \in (0,L)$. These trajectories find the target with the probability $\int_0^L dx_0 \, n_{\rm off}(x_0) \pi_L(x_0)$, where $\pi_L(x_0)$ is the splitting probability defined in Eq. (48). After evaluating the integral, Eq. (62) becomes

$$q = \frac{e^{-\alpha/2}}{2} \frac{\operatorname{erfi}\sqrt{\frac{\alpha}{2}} - \operatorname{erfi}\left(\sqrt{\frac{\alpha}{2}} - \sqrt{\frac{b^2}{2}}\right)}{\operatorname{erfi}\sqrt{\frac{b^2}{2}}},$$
 (63)

where $b = L/\sqrt{D\tau_K}$ and $\alpha = \tau_K/\tau$.

The mean time of a single unsuccessful trajectory to reach x = 0, designated by τ_{1-p} , is obtained from the following relation

$$(1-q)\tau_{1-p} = \int_0^L dx_0 \, n_{\text{off}}(x_0) t_0(x_0) + \int_{-\infty}^0 dx_0 \, n_{\text{off}}(x_0) t_{\text{on}}(x_0),$$
(64)

where $t_0(x_0)$ and $t_{\rm on}(x_0)$ have been defined and discussed previously. The second term represents trajectories that are prevented from reaching the target due to the location of the off switch at x = 0.

The mean time of a single successful trajectory is obtained from

$$q\tau_q = \int_L^{\infty} dx_0 \, n_{\text{off}}(x_0) t_q(x_0) + \int_0^L dx_0 \, n_{\text{off}}(x_0) t_L(x_0). \tag{65}$$

The expression distinguishes between different contributions. The first term represents trajectories with an initial point $x_0 \ge L$. All these trajectories will eventually find a target. The quantity $t_q(x_0)$ is the mean time to reach x = L for trajectories that start at x_0 . It satisfies the following differential equation [51]

$$1 = \mu K x_0 t_q'(x_0) - Dt_q''(x_0),$$

where the solultion for the boundary conditions $t_q(L) = 0$ is

$$t_q(x_0) = \frac{1}{D} \int_{L}^{x_0} dx e^{\mu K x^2 / 2D} \int_{x}^{\infty} dx' e^{-\mu K x'^2 / 2D}.$$
 (66)

The second term represents the trajectories with an initial point located in the interval $x_0 \in (0,L)$. The quantity $t_L(x_0)$ was already defined in Eq. (50).

After evaluating all the integrals involved in Eq. (61), we obtain the following compact expression in terms of previously defined quantities:

$$\tau_{sr} = \frac{\tau_{\rm on}}{q} - t_{\rm on}(L),\tag{67}$$

where $t_{\rm on}(x_0)$ is defined in Eq. (23), $\tau_{\rm on}$ in Eq. (22), and q is given by the formula in Eq. (63).

The simplicity and elegance of Eq. (67) invite physical interpretation. Both time scales describe the mean time a particle needs to reach the origin. The first term, τ_{on} , is the average over all possible initial positions x_0 , while the second term, $t_{on}(L)$, corresponds to the mean time from the position of the target, $x_0 = L$. It would be essentially impossible to deduce this relation from physical intuition alone. Its unusual structure strongly suggests that it arises from a sequence of mathematical cancellations within the derivation.

4. results

To confirm the analytical expressions, in Fig. (7) we plot the MFPT obtained from Eq. (67) and compare it with numerical simulations. The close agreement between the two confirms the validity of the theoretical framework.

In Fig. (8), we show τ_{sr} as a function of the waiting time τ for several values of the trap stiffness K, comparing the SRC and SR protocols. For small K, the SR protocol yields a lower MFPT, i.e., $\tau_{sr}^{SR} < \tau_{sr}^{SR-C}$, except in the regime of small τ , where τ_{sr}^{SR} diverges while τ_{sr}^{SR-C} approaches a finite limit, consistent with Eq. (55). As K increases, however, the SR-C protocol becomes more efficient and eventually outperforms SR-B across the entire range of τ .

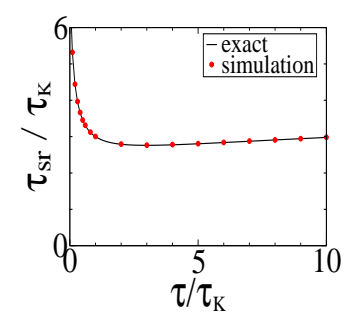


FIG. 7. MFPT as a function of τ for the SR-C protocol, comparing the analytical expression from Eq. (61) with data from numerical simulations. Parameters: $b = L/\sqrt{D\tau_K} = 1/\sqrt{0.3}$.

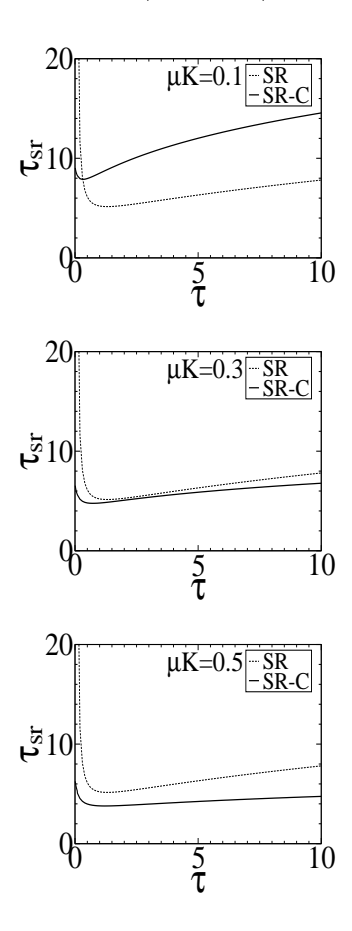


FIG. 8. MFPT as a function of τ for the SR-C protocol (solid lines) compared with the SR protocol (dashed lines), for three values of stiffness K. Parameters: L = 1, D = 0.3.

The dependence of τ_{sr} on trap stiffness K is further illustrated in Fig. (9), where τ_{sr} is plotted for a fixed $\tau = 1$. Since both τ and D are held constant, the initial distribution of return positions x_0 is independent of K, following $n_{\rm off}(x_0) \propto \exp(-|x_0|/\sqrt{D\tau})$. Thus, any variation in MFPT arises purely from the dynamics of the return trajectories. As K increases, particles are drawn more strongly toward the center by the trap, resulting in shorter return times and a more efficient search process.

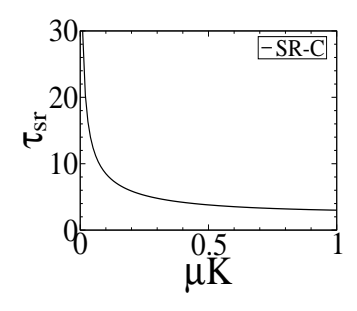


FIG. 9. MFPT τ_{sr} as a function of trap stiffness K for the SR-C protocol. Parameters: $\tau = 1, L = 1, D = 0.3$.

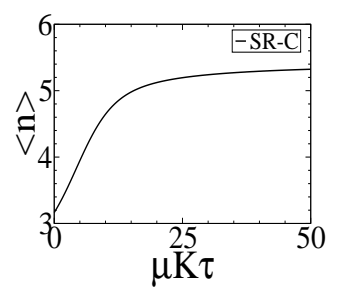


FIG. 10. Mean number of generations $\langle n \rangle = q_c^{-1}$ required to find the target, as a function of trap stiffness K. Parameters: $\tau=1,\,L=1,\,D=0.3$.

To better understand the mechanism underlying this reduction in τ_{sr} , Fig. (10) shows the mean number of generations required to locate the target, $\langle n \rangle = q^{-1}$, as a function of K. At first glance, it may seem paradoxical that $\langle n \rangle$ increases with stiffness—suggesting a less efficient search—seemingly contradicting the behavior observed in Fig. (9).

This apparent contradiction is resolved by analyzing the structure of the initial distribution $n_{\rm off}(x)$, which divides the population of return trajectories into two groups: a fraction $\int_L^\infty dx \, n_{\rm off}(x)$ originates on the "far side" of the target $(x_0 > L)$, and the remainder on the "near side" $(x_0 < L)$. As K increases, the steeper potential makes it harder for particles from $x_0 < L$ to reach the target, thus reducing their success probability. In contrast, all particles from $x_0 > L$ are deterministically pulled toward the target and will eventually cross it.

Fig. (11) confirms that although $\langle n \rangle = q^{-1}$ increases with trap stiffness K, the two characteristic time scales of the SR-C protocol, τ_q and τ_{1-p} , both decrease. This explains the overall reduction of the MFPT with increasing K as due to the greater search efficiency of particles originating on the "far side" of the target $(x_0 > L)$, which are driven deterministically toward the target by the stronger restoring force.

In the SR-C protocol, we introduce an additional control parameter: the trap stiffness K. As a result, the value of τ^* that minimizes the search time $\tau_{\rm sr}$, defined by

$$\left. \frac{d\tau_{\rm sr}}{d\tau} \right|_{\tau = \tau^*} = 0,\tag{68}$$

becomes a function of K. In Fig. (12), we plot this optimal value τ^* as a function of the dimensionless control parameter

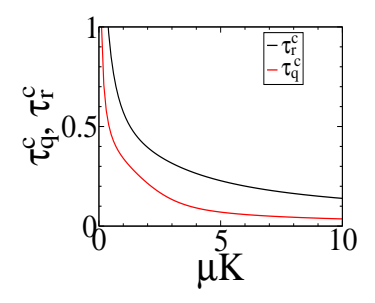


FIG. 11. The success probability q_c as a function of trap stiffness K for the SR-C protocol. Parameters: $L/\sqrt{D\tau} = 1$.

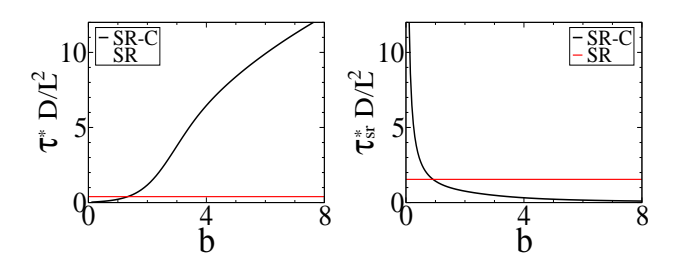


FIG. 12. The left panel shows the optimal reset time τ^* , corresponding to the minimum of $\tau_{\rm Sr}$, as a function of the control parameter $b=\sqrt{\mu K L^2/D}$. The right panel shows the corresponding minimal mean first-passage time $\tau_{\rm Sr}^*=\tau_{\rm Sr}(\tau^*)$. The red line represents the constant values obtained for the standard SR protocol, which does not depend on K.

 $b = L/\sqrt{D\tau_K} = \sqrt{\mu K L^2/D}$. The plot on the right-hand side indicates that we can bring τ_{sr} to an arbitrary low value by increasing K. The plot on the left-hand side indicates that the corresponding optimal τ^* shifts toward larger values, indicating that we need an increasingly broader distribution of initial points x_0 (since τ controls the distribution $n_{\rm off}$) with increasing K.

IV. CONCLUSION

In this work, we examined a fluctuating harmonic potential as a physical realization of stochastic resetting. By enforcing that all return trajectories terminate at the origin, we ensured a well-defined and reproducible starting point for each search cycle, thereby preserving a key structural assumption of the standard SR framework.

A distinctive feature of our model is the use of *information* to determine the precise moment at which the trap is switched off. This feedback shortens the duration of return trajectories without incurring additional mechanical energetic cost. In this respect, our setup falls within the class of Maxwell-demon–type models, where information is used to obtain an operational advantage—here, a reduction of return time.

Building on this controlled setting, we analyzed several search protocols that incorporate the return dynamics explicitly. To compute the mean first passage time (MFPT), we decomposed each cycle into statistically defined generations and expressed the relevant time scales and probabilities within a splitting-probability framework.

A particularly notable case is the protocol in which outward excursions are eliminated entirely and the search is performed solely through return motion. This inversion of the conventional outward-diffusion viewpoint yields an MFPT that can be written in closed form using the previously defined timescale parameters. Under strong confinement, this return-only protocol becomes more efficient than standard SR—not because individual return trajectories are inherently more effective, but because they are significantly faster.

ACKNOWLEDGMENTS

D.F. acknowledges financial support from FONDECYT through grant number 1241694.

V. DATA AVAILABILITY

The data that support the findings of this study are available from the corresponding author upon reasonable request.

^[1] M. Luby, A. Sinclair, and D. Zuckerman, Information Processing Letters 47, 173 (1993).

^[2] A. Montanari and R. Zecchina, Physical Review Letters 88, 178701 (2002).

^[3] O. Benichou, M. Coppey, M. Moreau, P.-H. Suet, and R. Voituriez, Physical Review Letters 94, 198101 (2005).

^[4] M. A. Lomholt, K. Tal, R. Metzler, and J. Klafter, Proceedings of the National Academy of Sciences 105, 11055 (2008).

^[5] M. R. Evans and S. N. Majumdar, Phys. Rev. Lett. 106, 160601 (2011)

^[6] M. R. Evans and S. N. Majumdar, Journal of Physics A: Mathematical and Theoretical 46, 185001 (2013).

^[7] J. Whitehouse, M. R. Evans, and S. N. Majumdar, Phys. Rev. E 87, 022118 (2013).

^[8] M. R. Evans and S. N. Majumdar, Journal of Physics A: Mathematical and Theoretical 47, 285001 (2014).

^[9] S. Gupta, S. N. Majumdar, and G. Schehr, Phys. Rev. Lett. 112, 220601 (2014).

^[10] X. Durang, M. Henkel, and H. Park, J. Phys. A: Math. Theor. 47, 045002 (2014).

^[11] L. Kusmierz, S. N. Majumdar, S. Sabhapandit, and G. Schehr, Phys. Rev. Lett. 113, 220602 (2014).

^[12] A. Pal, Phys. Rev. E 91, 012113 (2015).

- [13] S. N. Majumdar, S. Sabhapandit, and G. Schehr, Phys. Rev. E 92, 052126 (2015).
- [14] C. Christou and A. Schadschneider, J. Phys. A: Math. Theor. 48, 285003 (2015).
- [15] A. Pal, A. Kundu, and M. R. Evans, J. Phys. A: Math. Theor. 49, 225001 (2016).
- [16] S. Reuveni, Phys. Rev. Lett. 116, 170601 (2016).
- [17] R. Falcao and M. R. Evans, Journal of Statistical Mechanics: Theory and Experiment, 023204 (2017).
- [18] A. Pal and S. Reuveni, Phys. Rev. Lett. 118, 030603 (2017).
- [19] A. Pal, S. Kostinski, and S. Reuveni, Journal of Physics A: Mathematical and Theoretical 55, 021001 (2022).
- [20] M. R. Evans, S. N. Majumdar, and G. Schehr, Journal of Physics A: Mathematical and Theoretical 53, 193001 (2020).
- [21] S. Gupta and A. M. Jayannavar, Frontiers in Physics 10, 789097 (2022).
- [22] A. Pal, V. Stojkoski, and T. Sandev, in *Target Search Problems*, edited by D. Grebenkov, R. Metzler, and G. Oshanin (Springer, Cham, 2024).
- [23] O. Tal-Friedman, A. Pal, A. Sekhon, S. Reuveni, and Y. Roichman, The Journal of Physical Chemistry Letters 11, 7350 (2020).
- [24] R. Vatash, O. K. Damavandi, R. Klein, S. Reuveni, and Y. Roichman, Physical Review Letters 134, 057101 (2025).
- [25] B. Besga, A. Bovon, A. Petrosyan, S. N. Majumdar, and S. Ciliberto, Phys. Rev. Res. 2, 032029 (2020).
- [26] D. Gupta, C. A. Plata, A. Kundu, and A. Pal, Journal of Physics A: Mathematical and Theoretical 54, 025003 (2020).
- [27] D. Gupta, A. Pal, and A. Kundu, Journal of Statistical Mechanics: Theory and Experiment 2021, 043202 (2021).
- [28] I. Santra, S. Das, and S. K. Nath, Journal of Physics A: Mathematical and Theoretical 54, 334001 (2021).
- [29] H. Alston, L. Cocconi, and T. Bertrand, Journal of Physics A: Mathematical and Theoretical 55, 274004 (2022).
- [30] M. Biroli, M. Kulkarni, S. N. Majumdar, and G. Schehr, Phys. Rev. E 109, L032106 (2024).
- [31] D. Frydel, Phys. Rev. E 110, 024613 (2024).
- [32] S. Mukherjee and N. R. Smith, Journal of Statistical Mechanics: Theory and Experiment, 033205 (2025).
- [33] A. Biswas, A. Kundu, and A. Pal, Phys. Rev. E 110, L042101 (2024).

- [34] A. Biswas, A. Dubey, A. Kundu, and A. Pal, Phys. Rev. E 111, 014142 (2025).
- [35] G. Pesce, G. Volpe, A. Sasso, G. Volpe, and E. Arlt, European Physical Journal Plus 135, 949 (2020).
- [36] A. Kumar and J. Bechhoefer, in *Proceedings of SPIE*, Vol. 10723 (2018) p. 107230S.
- [37] S. Ghosh, A. Ghosh, M. Schäfer, and P. Fischer, Nature Communications 10, 2054 (2019).
- [38] C. Prohm, A. Zöttl, and H. Stark, Physical Review E 87, 045302 (2013).
- [39] A. Würger, Reports on Progress in Physics 73, 126601 (2010).
- [40] J. Dobnikar, A. Snezhko, and I. S. Aranson, Soft Matter 4, 1835 (2008).
- [41] A. Nagar and S. Gupta, Journal of Physics A: Mathematical and Theoretical 56, 383002 (2023).
- [42] S. N. Majumdar, A. Pal, and G. Schehr, Physics Reports 840, 1 (2020), extreme value statistics of correlated random variables: A pedagogical review.
- [43] I. A. Martínez, A. Petrosyan, D. Guéry-Odelin, E. Trizac, and S. Ciliberto, Nature Physics 12, 843 (2016).
- [44] T. Sagawa and M. Ueda, Phys. Rev. Lett. 104, 090602 (2010).
- [45] A. Archambault, C. Crauste-Thibierge, A. Imparato, C. Jarzynski, S. Ciliberto, and L. Bellon, Phys. Rev. Lett. 135, 147101 (2025).
- [46] J. M. R. Parrondo, J. M. Horowitz, and T. Sagawa, Nature Physics 11, 131 (2015).
- [47] F. Mori, K. S. Olsen, and S. Krishnamurthy, Phys. Rev. Res. 5, 023103 (2023).
- [48] J. Fuchs, S. Goldt, and U. Seifert, Europhysics Letters 113, 60009 (2016).
- [49] A. Pal and S. Rahav, Phys. Rev. E 96, 062135 (2017).
- [50] D. Gupta, C. A. Plata, and A. Pal, Phys. Rev. Lett. 124, 110608 (2020).
- [51] S. Redner, A Guide to First-Passage Processes (Cambridge University Press, Cambridge, 2001).
- [52] P. Chelminiak, arXiv preprint arXiv:2412.03165 (2024).
- [53] A. Pal and S. Reuveni, Physical Review E **99**, 032123 (2019).
- [54] A. Pal and S. Reuveni, Physical Review Letters 120, 020602 (2018).
- [55] J. Masoliver and M. Montero, Journal of Chemical Physics 159, 064117 (2023).